CHAPTER 11
STATISTICAL METHODS FOR ANALYZING VIBRATING SYSTEMS

Richard G. DeJong

INTRODUCTION

This chapter presents statistical methods for analyzing vibrating systems. Two situations often occur in which a statistical analysis is useful. The first occurs when the excitation of a system appears to be random in time, in which case it is convenient to describe the temporal response of the system statistically rather than deterministically. This form of analysis is called *random vibration analysis*[1] and is presented in the first half of this chapter. The second situation occurs when a system is complicated enough that its resonant modes appear to be distributed randomly in frequency, in which case it is convenient to describe the frequency response of the system statistically rather than deterministically. This form of analysis[2] is called *statistical energy analysis* (SEA) and is presented in the second half of this chapter.

In either situation the randomness need only appear to be so. For example, in random vibration it may be that the excitation could be calculated exactly if enough information were known. However, if the excitation is adequately described by statistical parameters (such as the *mean value* and *variance*), then a statistical analysis of the system response is valid. Similarly, in a complicated system the modes can presumably be analyzed deterministically. However, if the modal distribution is adequately described by statistical parameters, then a statistical energy analysis of the system response is valid whether or not the excitation is random.

RANDOM VIBRATION ANALYSIS

A random vibration is one whose instantaneous value is not predictable with the available information. Such vibration is generated, for example, by rocket engines, turbulent flows, earthquakes, and motion over irregular surfaces. While the instantaneous vibration level is not predictable, it is possible to describe the vibration in sta-

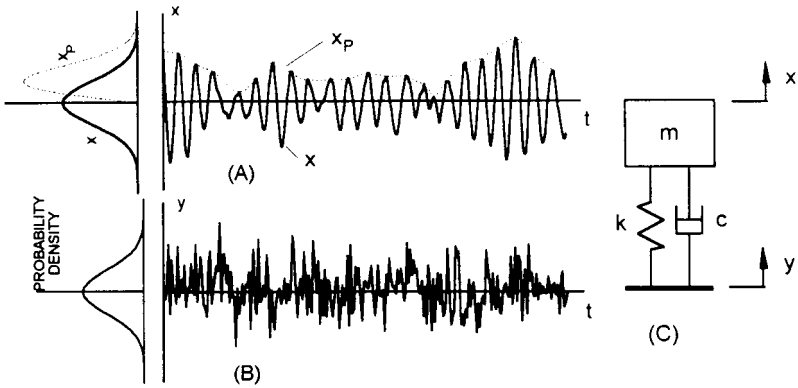

FIGURE 11.1 (*A*) Example of a narrow-band random signal $x(t)$ with a peak envelope x_p. (*B*) Example of a broad-band random signal $y(t)$. Curves along the vertical axes give the probability distributions for the instantaneous (solid lines) and peak (dashed line) values. (*C*) Resiliently mounted mass m with stiffness k and viscous damper c. When the base is exposed to a broad-band random vibration the mass will have a narrow-band random response.

tistical terms, such as the probability distribution of the vibration amplitude, the mean-square vibration level, and the average frequency spectrum.

A random process may be categorized as *stationary* (steady-state) or *nonstationary* (transient). A stationary random process is one whose characteristics do not change over time. For practical purposes a random vibration is stationary if the mean-square amplitude and frequency spectrum remain constant over a specified time period. A random vibration may be *broad-band* or *narrow-band* in its frequency content. Figure 11.1 shows typical acceleration-time records from a system with a mass resiliently mounted on a base subjected to steady, turbulent flow. The base vibration is broad-band with a *Gaussian* (or normal) amplitude distribution. The vibration of the mass is narrow-band (centered at the natural frequency of the mounted system) but also has a Gaussian amplitude distribution. The peaks of the narrow-band vibration have a distribution called the *Rayleigh* distribution.

Technically, the statistical measures of a random process must be averaged over an *ensemble* (or assembly) of representative samples. For an arbitrary random vibration this means averaging over a set of independent realizations of the event. This is illustrated in Fig. 11.2 where four vibration-time records from a point on an internal combustion engine block are shown synchronized with the firing in a particular cylinder. Due to uncontrollable variations in the system, the vibration is not deterministically repeatable. The mean-square amplitude is also nonstationary. Therefore, the statistical parameters of the vibration are time dependent and must be determined from the ensemble of samples from each record at a particular time.

For a stationary random process it may be possible to obtain equivalent ensemble averages by sampling over time if each time record is representative of the entire random process. Such a random process is called *ergodic.* However, not all stationary random processes are ergodic. For example, suppose it is desired to determine the statistical parameters of the vibration levels of an aircraft fuselage during representative in-flight conditions. On a particular flight the vibration levels may be sufficiently stationary to obtain useful time averages. However, one flight is unlikely to encompass all of the expected variations in the weather and other conditions that affect the vibration levels. In this case it is necessary to combine the time averages with an ensemble average over a number of different flight conditions which represent the entire range of possible conditions.

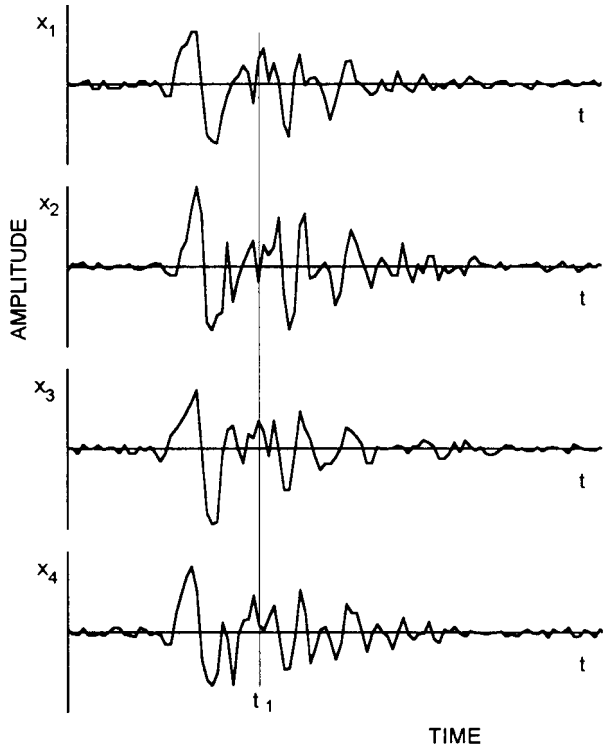

FIGURE 11.2 Ensemble of vibration responses (x_1, x_2, x_3, x_4) measured at a point on an internal combustion engine block and synchronized with a particular cylinder firing. The amplitude at time t_1 is a random variable.

The first half of this chapter describes methods for determining the response of a vibrating system subjected to random excitations. First, the statistical parameters used in this analysis are presented. Next, the responses of single and multiple degree-of-freedom systems to random excitations (stationary and nonstationary) are analyzed. Then, the application of this analysis to failure prediction is summarized. (More information on failure analysis is included in Chap. 34.)

*STATISTICAL PARAMETERS OF RANDOM VIBRATIONS**

PROBABILITY DISTRIBUTION FUNCTIONS

The fundamental statistical parameter of a random vibration is the probability distribution of the vibration amplitude $x(t)$ as a function of time. (In general, x may represent the acceleration, velocity, displacement, stress, etc.) In Fig. 11.1 the amplitude

* See Chap. 22 for methods to determine these parameters from measured data.

distribution of x is represented by the *probability density function* $p(x)$. The function $p(x)$ is obtained from the probability that a particular sample $x_i(t_1)$ has a value between x and $x + \Delta x$, represented by $\text{Prob}[x \le x_i(t_1) < x + \Delta x]$. For a nonstationary random process this probability is a function of the time t_1. The probability density is defined by

$$p(x,t_1) \equiv \lim_{\Delta x \to 0} \frac{\text{Prob}[x \le x_i(t_1) < x + \Delta x]}{\Delta x} \tag{11.1}$$

An alternate representation of the amplitude distribution is the *cumulative* (*probability*) *distribution function* $P(x)$, which is the probability that a particular sample $x_i(t_1)$ has a value less than or equal to x. The cumulative distribution is defined by

$$P(x,t_1) \equiv \text{Prob}[x_i(t_1) \le x] = \int_{-\infty}^{x} p(x',t_1)\, dx' \tag{11.2}$$

Therefore, the probability density and cumulative distribution functions are related as illustrated in Fig. 11.3. For most random processes the cumulative distribution function is smooth and differentiable so that Eq. (11.2) can be rewritten as

$$p(x,t_1) = \frac{d}{dx} P(x,t_1) \tag{11.3}$$

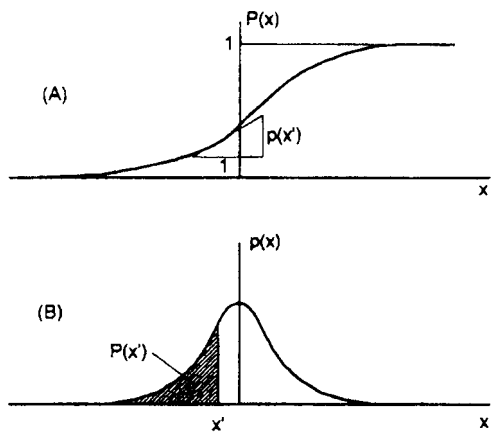

FIGURE 11.3 Examples of the probability distributions of a random variable x. (*A*) Cumulative (probability) distribution function, $P(x)$. (*B*) Probability density function $p(x)$.

Since by definition $P(x) \to 1$ as $x \to \infty$, the total area under $p(x)$ is normalized to be unity, or

$$P(\infty,t_1) = \int_{-\infty}^{\infty} p(x,t_1)\, dx = 1 \tag{11.4}$$

MEAN VALUE

The *mean* (or expected) *value* $\overline{x(t_1)}$ of x at time t_1 is defined by the arithmetic average of all samples $x_i(t_1)$:

$$\overline{x(t_1)} \equiv \lim_{N \to \infty} \frac{1}{N} \sum_{i=1}^{N} x_i(t_1) \tag{11.5}$$

The mean value can be obtained from the probability density by

$$\overline{x(t_1)} = \int_{-\infty}^{\infty} x p(x,t_1)\, dx \tag{11.6}$$

If $x(t)$ is stationary over time $0 \le t \le T$, then the mean value can be approximated by the time average:

$$\bar{x} \simeq \frac{1}{T} \int_0^T x(t)\, dt \tag{11.7}$$

where the approximation improves as $T \to \infty$.

MEAN-SQUARE VALUE

The *mean-square value* $\overline{x^2(t_1)}$ is defined as the expected value of all samples $x_i^2(t_1)$. The mean-square value can be obtained from the probability density by

$$\overline{x^2(t_1)} = \int_{-\infty}^{\infty} x^2\, p(x,t_1)\, dx \tag{11.8}$$

If $x(t)$ is stationary, then the mean-square value can be approximated by the time average:

$$\overline{x^2} \simeq \frac{1}{T} \int_0^T x^2\,(t)\, dt \tag{11.9}$$

MOMENTS OF THE PROBABILITY DISTRIBUTION

The mean and mean-square values are called the first and second moments of $p(x)$, respectively. The nth moment of $p(x)$ is then defined by

$$\overline{x^n(t_1)} = \int_{-\infty}^{\infty} x^n\, p(x,t_1)\, dx \tag{11.10}$$

The *variance* σ^2 (or square of the *standard deviation* σ) is the expected value of the quantity $(x - \bar{x})^2$ and is evaluated by

$$\sigma^2 = \int_{-\infty}^{\infty} (x - \bar{x})^2\, p(x)\, dx = \overline{x^2} - (\bar{x})^2 \tag{11.11}$$

where the designation of the time dependence is omitted for clarity. The variance is then the difference between the mean-square and the square of the mean value of x.

For many random variables in vibration analysis the mean value is zero so that the variance and mean-square values can be used interchangeably.

Higher-order moments are usually represented in terms of the normalized variable $z = (x - \bar{x})/\sigma$. The value of z is the number of standard deviations x is from the mean. The normalized third moment is called the *skewness* a_3:

$$a_3 = \int_{-\infty}^{\infty} \left(\frac{x - \bar{x}}{\sigma} \right)^3 p(x)\, dx \tag{11.12}$$

The normalized fourth moment is called the *kurtosis* a_4:

$$a_4 = \int_{-\infty}^{\infty} \left(\frac{x - \bar{x}}{\sigma} \right)^4 p(x)\, dx \tag{11.13}$$

For a Gaussian distribution $a_3 = 0$ and $a_4 = 3$.

GAUSSIAN (NORMAL) DISTRIBUTION

The Gaussian distribution is important in random vibration analysis because it is so frequently encountered. The Gaussian probability density function is given by

$$p(x) = \frac{1}{\sigma\sqrt{2\pi}}\, e^{-1/2[(x - \bar{x})/\sigma]^2} \tag{11.14}$$

One reason the Gaussian distribution is so common is the *central limit theorem* which states that the sum of N random variables having an arbitrary distribution will approach a Gaussian distribution as $N \to \infty$. If a random vibration results from the sum of a large number of random excitations, its distribution will tend to be Gaussian.

As a corollary to this, if a vibration response results from the product of a large number of random variables, the logarithm of the vibration magnitude will be the sum of the logarithm of the variables, and this sum will tend to have a Gaussian distribution. The vibration magnitude is then said to have a *log-normal* distribution. This occurs in the vibration of complex machinery where the distribution of responses over an ensemble of nominally identical units will tend to be log-normal.

One common model for the excitation of a random vibration is a sequence of pulses with random amplitudes and random time spacing as illustrated in Fig. 11.4. This model can represent, for example, the pressure pulses in the boundary layer of a turbulent fluid flow or the sequence of stress pulses from an earthquake arriving at some location after propagating through the earth's stratified media. The response of a system to this type of excitation can be thought of as a sum of the responses to each pulse. The response of a system to a unit impulse is called the *impulse response* $h(t)$. The response to a sequence of pulses is then the sum of a sequence of impulse responses appropriately scaled in amplitude and delayed in time. If the impulse response is long compared to the average spacing between the pulses, then the resulting system response will have a Gaussian distribution.

Broad-band, stationary random variables with Gaussian distributions are often called *white noise.* Ideally, white noise has an equal contribution from all frequencies. Practically, white noise is usually band-limited to the frequency range of interest. However, a Gaussian distribution does not necessarily imply white noise. This can be seen from Fig. 11.1 where the vibration response of the resiliently mounted mass is Gaussian and narrow-band in frequency.

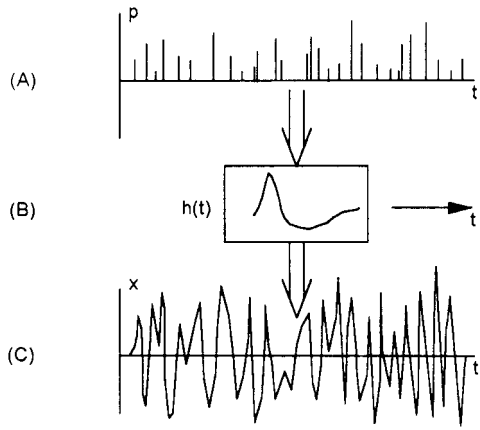

FIGURE 11.4 Example of the generation of broadband random vibration with a Gaussian probability distribution. (*A*) Sequences of excitation pulses *p.* (*B*) System impulse response function $h(t)$. (*C*) Resulting system response amplitude x.

CORRELATION FUNCTIONS

Correlation functions are used to describe the average relation between random variables. The *autocorrelation* $R_{xx}(\tau)$ is the expected value of the product of two samples of $x_i(t)$ that are separated in time by τ. In general, the autocorrelation is a function of the time t_1 of the first sample:

$$R_{xx}(\tau,t_1) = \overline{x(t_1)x(t_1+\tau)} \tag{11.15}$$

By definition the autocorrelation at zero delay ($\tau = 0$) is equal to the mean-square value of the variable, and this is the maximum value of the autocorrelation function.

If $x(t)$ is stationary over time $0 \le t \le 2T$, the autocorrelation is independent of the time of the first sample and is a function only of the absolute value of the delay τ. Then, the autocorrelation function (for $0 \le \tau \le T$) can be approximated by the time average:

$$R_{xx}(-\tau) = R_{xx}(\tau) \simeq \frac{1}{T}\int_0^T x(t)x(t+\tau)\,dt \tag{11.16}$$

Comparing Eqs. (11.9) and (11.16) it follows that $R_{xx}(0) = \overline{x^2}$.

For a system excited by white noise the autocorrelation of a response variable can be used to determine the frequency bandwidth of the system response function. If white noise is filtered with an ideal bandpass filter having cut-off frequencies f_1 and f_2 ($f_1 < f_2$), the autocorrelation of the resulting band-limited random variable is given by

$$R_{xx}(\tau) = \overline{x^2}\frac{\sin(2\pi f_2\tau) - \sin(2\pi f_1\tau)}{2\pi(f_2 - f_1)\tau} \tag{11.17}$$

If $f_1 = 0$, the first zero crossing of the autocorrelation function occurs at a delay $\tau = 1/f_2$.

The average relation between two variables $x(t)$ and $y(t)$ is represented by the *cross-correlation* $R_{xy}(\tau,t_1)$ defined by

$$R_{xy}(\tau,t_1) = \overline{x(t_1)y(t_1+\tau)} \tag{11.18}$$

For variables of a stationary process, the cross-correlation is a function only of the delay τ. However, the maximum value does not necessarily occur at $\tau = 0$. The cross-correlation function can be approximated by the time average:

$$R_{xy}(\tau) \simeq \frac{1}{T}\int_0^T x(t)y(t+\tau)\,dt \tag{11.19}$$

POWER SPECTRAL DENSITY

The frequency content of a random variable $x(t)$ is represented by the *power spectral density* $W_x(f)$, defined as the mean-square response of an ideal narrow-band filter to $x(t)$, divided by the bandwidth Δf of the filter in the limit as $\Delta f \to 0$ at frequency f (Hz):

$$W_x(f) = \lim_{\Delta f \to 0} \frac{\overline{x_{\Delta f}^2}}{\Delta f} \tag{11.20}$$

This is illustrated in Fig. 22.5. By this definition the sum of the power spectral components over the entire frequency range must equal the total mean-square value of x:

$$\overline{x^2} = \int_0^\infty W_x(f)\,df \tag{11.21}$$

The term *power* is used because the dynamical power in a vibrating system is proportional to the square of the vibration amplitude.

An alternate approach to the power spectral density of stationary variables uses the *Fourier series* representation of $x(t)$ over a finite time period $0 \le t \le T$, defined in Eq. (22.4) as

$$x(t) = \bar{x} + \sum_{n=1}^{\infty} A_n \cos(2\pi f_n t) + \sum_{n=1}^{\infty} B_n \sin(2\pi f_n t) \tag{11.22}$$

where $f_n = n/T$. The coefficients of the Fourier series are found by

$$\begin{aligned} A_n &= \frac{2}{T}\int_0^T x(t)\cos(2\pi f_n t)\,dt \\ B_n &= \frac{2}{T}\int_0^T x(t)\sin(2\pi f_n t)\,dt \end{aligned} \tag{11.23}$$

Comparing this to Eq. (11.19), it follows that the coefficients of the Fourier series are a measure of the correlation of $x(t)$ with the cosine and sine waves at a particular frequency.

The relation between the Fourier series and the power spectral density can be found by evaluating $\overline{x^2}$ from Eq. (11.22):

$$\overline{x^2} = \frac{1}{T}\int_0^T \left\{ \bar{x} + \sum_{n=1}^{\infty} [A_n \cos(2\pi f_n t) + B_n \sin(2\pi f_n t)] \right\} \times \left\{ \bar{x} + \sum_{m=1}^{\infty} [A_m \cos(2\pi f_m t) + B_m \sin(2\pi f_m t)] \right\} dt \qquad (11.24)$$

The integral over time cancels all cross terms in the product of the Fourier series leaving only the squares of each term:

$$\overline{x^2} = \frac{1}{T}\int_0^T \left\{ (\bar{x})^2 + \sum_{n=1}^{\infty} [A_n^2 \cos^2(2\pi f_n t) + B_n^2 \sin^2(2\pi f_n t)] \right\} dt$$

$$= (\bar{x})^2 + \sum_{n=1}^{\infty} \frac{1}{2}\left[A_n^2 + B_n^2 \right] \qquad (11.25)$$

Each term in this series can be viewed as representing a component of the mean-square value associated with a filter of bandwidth $\Delta f = 1/T$. The power spectral density is then approximated by

$$W_x(f_n) \simeq \frac{T}{2}\left(A_n^2 + B_n^2 \right) \qquad (11.26)$$

Using a similar method the relation between $W_x(f)$ and $R_{xx}(\tau)$ can be found. Equation (11.24) can be used to evaluate $R_{xx}(\tau)$ by changing the factors $f_m t$ to $f_m(t + \tau)$. The time integration removes all terms except those of the form $\frac{1}{2}(A_n^2 + B_n^2)\cos(2\pi f_n \tau)$. The autocorrelation is then given by

$$R_x(\tau) = (\bar{x})^2 + \sum_{n=1}^{\infty} \frac{1}{2}\left(A_n^2 + B_n^2 \right)\cos(2\pi f_n \tau)$$

$$= (\bar{x})^2 + \sum_{n=1}^{\infty} W_x(f_n)\cos(2\pi f_n \tau)\Delta f \qquad (11.27)$$

In the limit as $T \to \infty$, $\Delta f \to 0$ and the summation approaches the continuous integral:

$$R_x(\tau) = \int_0^{\infty} W_x(f)\cos(2\pi f \tau)\, df \qquad (11.28)$$

This is the Fourier cosine transform. The reciprocal relation is:

$$W_x(f) = 4\int_0^{\infty} R_x(\tau)\cos(2\pi f \tau)\, d\tau \qquad (11.29)$$

For transient random variables the power spectral density is a function of time. However, if the power spectral density is integrated over the time duration of a transient $x(t)$, an *energy spectral density* $E_x(f)$ can be obtained representing the frequency content of the total energy in x. Using the Fourier series approach, $E_x(f_n) = TW_x(f_n)$. Alternately, the *shock spectrum* can be used to represent the frequency content of a transient. The shock spectrum represents the peak amplitude response

of a narrow-band resonance filter to a transient event (see Chap. 23). A statistical method for estimating the shock spectrum is given in the next section.

RESPONSE OF A SINGLE DEGREE-OF-FREEDOM SYSTEM

In this section the single degree-of-freedom resonator shown in Fig. 11.1 is analyzed to obtain an expression for the mean-square response of the mass when the base is subjected to a random vibration. The equation of motion for this system is derived in Chap. 2 as

$$\ddot{z} + \frac{c}{m}\dot{z} + \frac{k}{m}z = \ddot{y} \tag{11.30}$$

where $z = x - y$ is the motion of the mass relative to the base. This equation is similar in form to the equation for a force excitation $F(t)$ on the mass and a rigid base:

$$\ddot{x} + \frac{c}{m}\dot{x} + \frac{k}{m}x = \frac{F(t)}{m} \tag{11.31}$$

In general, the equations of this form can be solved using r for the response variable and s for the source term. Defining

$$\begin{aligned} f_n &= \frac{1}{2\pi}\sqrt{\frac{k}{m}} = \text{the natural frequency} \\ \zeta &= \frac{c}{2\sqrt{km}} = \text{the critical damping ratio} \end{aligned} \tag{11.32}$$

gives:

$$\ddot{r} + 4\pi\zeta f_n \dot{r} + (2\pi f_n)^2 r = s(t) \tag{11.33}$$

With a sinusoidal acceleration source $s(t) = S\sin(2\pi ft)$, the relative displacement response of the system is given in terms of a *frequency response function* $H(f)$ with a magnitude given as

$$|H(f)|^2 = \frac{W_r(f)}{W_s(f)} = \frac{1}{(2\pi f_n)^4\left\{\left[1 - \left(\frac{f}{f_n}\right)^2\right]^2 + \left(2\zeta\frac{f}{f_n}\right)^2\right\}} \tag{11.34}$$

For a broad-band random source, if $\zeta << 1$ so that $|H(f)|^2$ is sharply peaked at $f = f_n$ and the source is stationary with a relatively smooth spectrum, as illustrated in Fig. 11.5, then the mean-square response of the system is determined by the source spectrum at $f = f_n$ times the area under the $|H(f)|^2$ curve:

$$\overline{r^2} = W_s(f_n)\int_0^\infty |H(f)|^2\, df = \frac{W_s(f_n)}{8\zeta(2\pi f_n)^3} \tag{11.35}$$

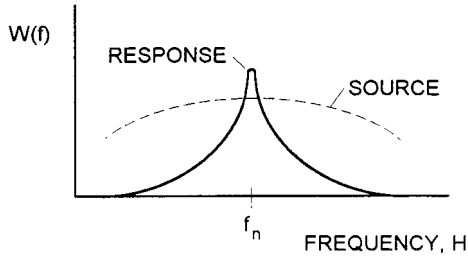

FIGURE 11.5 Power spectral density $W(f)$ of the response of a resonator with $\zeta << 1$ excited by a broad-band random source having the spectrum shown by the dashed curve.

The resonance of the system acts as a narrow-band filter on the source spectrum as is illustrated in Fig. 11.1. The vibration is essentially at frequency f_n with a Gaussian amplitude distribution. The mean-square acceleration and velocity levels are related to the displacement response by $\overline{\ddot{x}^2} = (2\pi f_n)^2\overline{\dot{x}^2} = (2\pi f_n)^4\overline{x^2}$. The autocorrelation of the stationary response is found to be

$$R_r(\tau) = \overline{r^2}\, e^{-2\pi\zeta f_n\tau}\left[\cos(2\pi f_d t) + \frac{\zeta}{\sqrt{1-\zeta^2}}\sin(2\pi f_d t)\right] \tag{11.36}$$

where $f_d = f_n\sqrt{1-\zeta^2}$.

The response of the resonator to a transient excitation can be analyzed for the simple case where the source is suddenly turned on and remains stationary thereafter.[3] The transient mean-square response starting from rest is then found to be (for $\zeta << 1$)

$$\overline{r^2}(t) = \frac{W_s(f_n)}{8\zeta(2\pi f_n)^3}\,(1 - e^{-4\pi\zeta f_n t}) \tag{11.37}$$

The mean-square response grows to the steady-state value in the same way that a first-order dynamic system responds to a step input. This is an important result, illustrating that the dynamical power in a vibrating system is transmitted according to the simple first-order diffusion equation with a time constant $\tau = 1/(4\pi\zeta f_n)$.

This result can be used to estimate the shock spectrum of a transient random excitation with a known time-dependent mean-square level $\overline{s^2}(t,\Delta f)$ in the frequency band Δf. The mean-square response of a resonator to this excitation can be found by solving the following first-order differential equation either numerically or using the Laplace transform method (see Chap. 8):

$$\frac{d}{dt}\overline{r^2}(t) + (4\pi\zeta f_n)\overline{r^2}(t) = \frac{\overline{s^2}(t)}{4\Delta f(2\pi f_n)^2} \tag{11.38}$$

assuming f_n is within the bandwidth Δf.

For example, Fig. 11.6 shows the measured transient acceleration of a concrete floor slab in a building with an operating punch press. As with many transient vibration time-histories, the smoothed mean-square level can be approximated by

$$\overline{\ddot{x}^2}(t) = At\, e^{-\beta t} \tag{11.39}$$

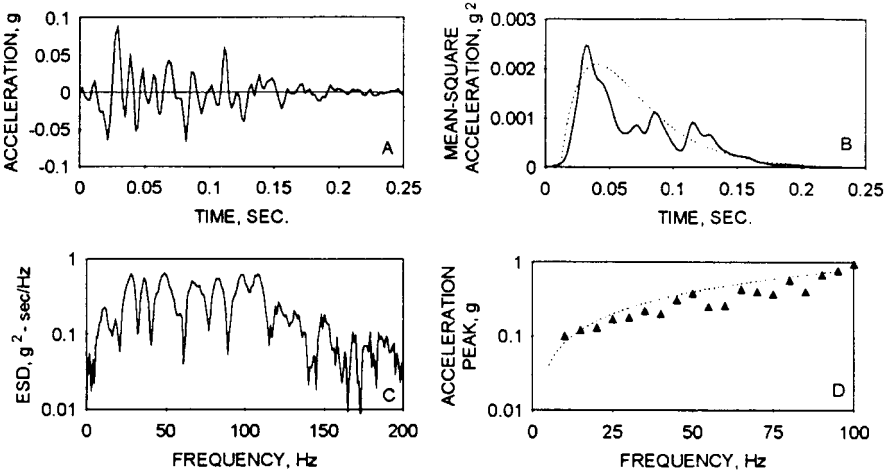

FIGURE 11.6 Transient response of a concrete floor slab with an operating punch press. (*A*) Measured acceleration signal. (*B*) Mean-square smoothed signal (solid curve) and curve fit (dashed curve) using Eq. (11.39). (*C*) Measured energy spectral density. (*D*) Computed acceleration shock response spectrum (symbols) and statistical estimate (dashed curve) using Eq. (11.42).

where for this case $A \simeq 0.2g^2/s$ and $\beta \simeq 35/s$ with $\Delta f \simeq 80$ Hz. The solution of Eq. (11.38) with this form of excitation is given by

$$\overline{r^2}(t) = \frac{A}{4\Delta f(2\pi f_n)^2}\left[\frac{t(\alpha-\beta)e^{-\beta t} + e^{-\alpha t} - e^{-\beta t}}{(\alpha-\beta)^2}\right] \tag{11.40}$$

where $\alpha = 4\pi\zeta f_n$. The undamped shock response is the maximum response level as $\alpha \to 0$, which is

$$\overline{r^2}_{\max} \to \frac{A}{4\Delta f(2\pi f_n)^2\beta^2} \tag{11.41}$$

The undamped shock response spectrum is the peak response as a function of f_n (see Chap. 23), which can be estimated with 95 percent certainty as the 2σ level assuming a Gaussian distribution:

$$r_{\text{peak}} \simeq 2\sqrt{\overline{r^2}_{\max}} = \sqrt{\frac{A}{\Delta f}}\,\frac{1}{2\pi f_n\beta} \tag{11.42}$$

This result is plotted in Fig. 11.6*D* along with the exact calculation of the shock spectrum at 5-Hz intervals using a particular sample of the acceleration time-history.

RESPONSE OF MULTIPLE DEGREE-OF-FREEDOM SYSTEMS

Real elastic systems have many degrees-of-freedom and, therefore, many modes of resonance, as discussed in Chaps. 2 and 7. However, these *normal modes* ψ_n each

respond as a simple resonator, and the total response of a system can be obtained by summing the response of all of the modes (*modal superposition*):

$$r(\upsilon,t) = \sum_n q_n(t)\psi_n(\upsilon) \tag{11.43}$$

where υ represents the spatial dimension(s) of the system.

If the damping in the system is distributed proportionately to the mass and stiffness, the normal modes are uncoupled and each has an equation of motion in the form of Eq. (11.33) with a source term given by

$$s_n(t) = \int s(\upsilon,t)\psi_n(\upsilon)\, d\upsilon \equiv \varphi_n \sqrt{\overline{s^2(\upsilon,t)}} \tag{11.44}$$

where φ_n is the modal participation factor of the source. The transfer function for each mode will be of the form of Eq. (11.34) so that the resulting sum of the modal responses gives

$$\overline{r^2} = \sum_n \frac{\varphi_n^2 \psi_n^2 W_s(f_n)}{8\zeta_n(2\pi f_n)^3} \tag{11.45}$$

If the damping is not distributed proportionately but is small ($\zeta << 1$), the superposition of normal modes gives approximately correct results. This is illustrated by the two degree-of-freedom system shown in Fig. 11.7. An instrument housing (m_1) is resiliently mounted on a vibrating base. A dynamic vibration absorber (see Chap. 6) is attached to suppress the vibration of the housing at frequency f_2. Of interest here is the broad-band response of the system when the base vibration has a uniform

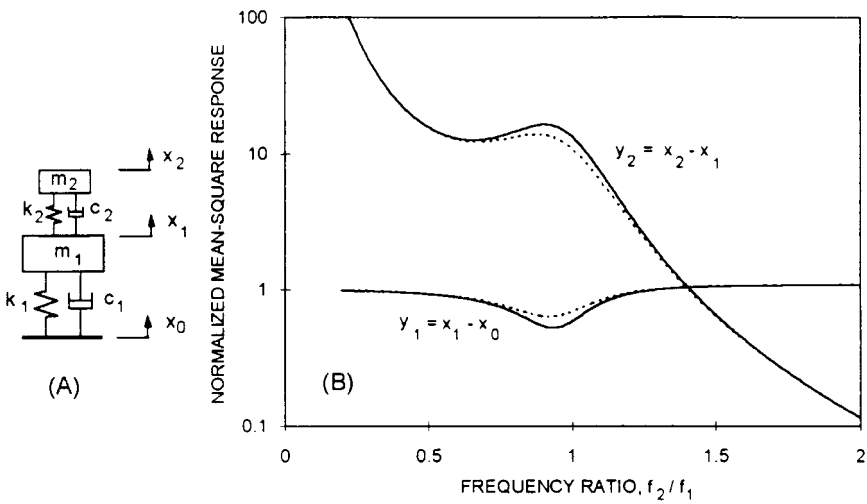

FIGURE 11.7 (*A*) Response of a two degree-of-freedom system to a base excitation x_0. (*B*) Mean-square relative displacement responses, y_1 and y_2, normalized to the response of m_1 alone. Solid curves are calculated using the modal summation of Eq. (11.45). Dashed curves are the exact calculations.

acceleration spectral density $W_{\ddot{x}_0}$. The equations for the relative responses $y_1 = x_1 - x_0$ and $y_2 = x_2 - x_1$ in symmetric, dimensionless form are

$$\begin{bmatrix} 1 & 0 \\ 0 & \dfrac{\mu f_2^2}{f_1^2} \end{bmatrix} \begin{Bmatrix} \ddot{y}_1 \\ \ddot{y}_2 \end{Bmatrix} + \begin{bmatrix} 4\pi\zeta_1 f_1 & -4\pi\mu\zeta_2 f_2 \\ -4\pi \dfrac{\mu f_2^2}{f_1^2}\zeta_1 f_1 & (1+\mu)\dfrac{\mu f_2^2}{f_1^2}(2\pi f_2)^2 \end{bmatrix} \begin{Bmatrix} \dot{y}_1 \\ \dot{y}_2 \end{Bmatrix}$$

$$+ \begin{bmatrix} (2\pi f_1)^2 & -\mu(2\pi f_2)^2 \\ -\mu(2\pi f_2)^2 & (1+\mu)\dfrac{\mu f_2^2}{f_1^2}(2\pi f_2)^2 \end{bmatrix} \begin{Bmatrix} y_1 \\ y_2 \end{Bmatrix} = \begin{Bmatrix} -\ddot{x}_0 \\ 0 \end{Bmatrix} \tag{11.46}$$

where $\mu = m_2/m_1$, $2\pi f_i = \sqrt{k_i/m_i}$ and $4\pi\zeta_i f_i = c_i/m_i$. The damping is symmetric only if $\zeta_1 f_2 = \zeta_2 f_1$.

Consider a specific example where $\mu = 0.04$ and $\zeta_1 = \zeta_2 = 0.05$, so the damping is not symmetric. Figure 11.7 shows the calculated values of the mean-square responses $\overline{y_1^2}$ and $\overline{y_2^2}$ as a function of f_2/f_1. The amplitudes are plotted relative to the mean-square response that m_1 would have without the attached vibration absorber $\overline{y_{1o}^2}$ as calculated using Eq. (11.35). The modal superposition calculation ignores the small cross-coupling between the normal modes due to the nonsymmetric damping. These results are compared to the exact solution for the two degree-of-freedom system.[1] The mean-square response of m_1 is suppressed only when $f_2 \simeq f_1$ and only by about 4 dB.

EVALUATION OF FAILURE CRITERIA

Random vibration can contribute to the fatigue and failure of systems. The vibration may contribute to the cyclical stress loading in a part of the system and accelerate the accumulation of fatigue or crack growth leading to eventual failure. Or, the vibration may increase the probability of exceeding the ultimate stress in a part of the system during its operation leading to immediate failure. Chapter 34 describes the analysis of failure mechanisms in more detail. This section presents methods to estimate the distribution of system response levels resulting from random vibration in forms that can be used in failure models. It is assumed that the stress levels induced by the vibration are linearly related to the relative displacement levels y in the system.

LEVEL CROSSINGS

The vibration responses of systems exposed to random excitations frequently have a Gaussian distribution over time. This is true of both broad-band and narrow-band vibration as illustrated in Fig. 11.1. Even if the excitation is not Gaussian, complex systems with many modes of vibration contributing to the total response will, by the central limit theorem, tend to have a Gaussian response distribution. The probability that the vibration response y will exceed a limiting value y_L is given by

$$P(y > y_L) = \int_{y_L}^{\infty} p(y)dy = \frac{1}{2}\,\mathrm{erfc}\left(\frac{y_L}{\sqrt{2}\sigma_y}\right) \tag{11.47}$$

where y is assumed to have a Gaussian distribution with zero mean and variance σ_y^2. The function erfc is the complimentary error function. For linear systems the distribution of random vibration levels can be superimposed on the static (or slowly varying) stress levels.

This distribution can be used to obtain an estimate of the rate of occurrence ν of a particular level crossing. The inverse of this rate is the mean time between occurrences of this level crossing. For a broad-band random vibration the rate of crossing the level $y = a$ with a positive slope, denoted by ν_a^+, is

$$\nu_a^+ = \frac{1}{2\pi} \frac{\sigma_{\dot{y}}}{\sigma_y} e^{-\frac{a^2}{2\sigma_y^2}} \tag{11.48}$$

For a narrow-band vibration $\sigma_{\dot{y}} = 2\pi f_n \sigma_y$, so the level crossing rate is simply

$$\nu_a^+ = f_n e^{-\frac{a^2}{2\sigma_y^2}} \tag{11.49}$$

Caution must be used when applying Eqs. (11.48) and (11.49) to values of $|a| > 2\sigma_y$. While many vibration distributions may be adequately represented by a Gaussian distribution in the range of $\pm 2\sigma$ from the mean, there may be significant deviations outside this range. This may cause significant errors in rate of crossing estimates for extreme values. Therefore, the rate of crossing estimates are not that useful for estimating the time to the first occurrence of a large stress resulting from a random vibration.

CUMULATIVE DAMAGE

The rate of occurrence estimates are more useful in a cumulative damage model which sums up the effects of repeated occurrences of excessive stress until a failure criteria is met. Often these failure models are based on the number of occurrences of peak levels in a cyclical loading pattern. This is true in the fatigue limit analysis using *S-N* curves and also in the fracture mechanics analysis using exceedance curves (see Chap. 34). For true white noise the peak levels have a Gaussian distribution. However, for band-limited Gaussian vibrations, the distribution of the peak levels is more complicated. For broad-band random vibrations the probability density function of the absolute level of the displacement peaks is found to be approximated by the Poisson (exponential) distribution

$$p(|y_P|) = \frac{1}{\sigma_y} e^{-|y_P|/\sigma_y} \tag{11.50}$$

For narrow-band vibrations the probability density function of the peaks is found to be approximated by the Rayleigh distribution (see Fig. 11.1)

$$p(|y_P|) = \frac{y_P}{\sigma_y^2} e^{-y_P/2\sigma_y} \tag{11.51}$$

These distributions of peak levels can be used with cyclical fatigue limit curves to estimate a measure of the cumulative damage D. For example, if a material *S-N* curve is approximated by $N = cS^{-b}$ (N equals the number of cycles to failure at a peak stress level S) and the critical stress is a function of the vibration displacement $S =$

$S(y)$, then the expected value of the accumulated damage over time by a random vibration is

$$\overline{D(t)} = v_0^+ t \int_0^\infty \frac{p(y_P)}{N(y_P)} dy_P \tag{11.52}$$

where failure occurs around $D(t) = 1$. With this analysis there is not only a statistical uncertainty due to variations in the material properties, but there is also an uncertainty in the distribution of vibration cycles. The variance in the estimate of $D(t)$ due to this latter uncertainty is estimated to be

$$\sigma_D^2 \simeq \overline{D}^2 \frac{10^{(b-5)/4}}{\zeta v_0^+ t} \qquad (b > 5) \tag{11.53}$$

for the narrow-band vibration case.

For estimates of crack propagation in fracture mechanics, an exceedance diagram is often used. The exceedance diagram plots the peak stress level as a function of the number of cycles which exceed this stress level. The exceedance curve in a random vibration is then found from the cumulative distribution function of the peak levels. For a broad-band limited vibration,

$$P(|y_P| > y_L) = e^{-y_L/\sigma_y} \tag{11.54}$$

and for a narrow-band vibration,

$$P(|y_P| > y_L) = e^{-y_L^2/2\sigma_y^2} \tag{11.55}$$

These probability functions are shown in the form of exceedance curves in Fig. 11.8 with the relative amplitude y_P/σ_y plotted as a function of the logarithm of P. The number of cycles N occurring in time t can be found by multiplying P by the appropriate value of $v_0^+ t$.

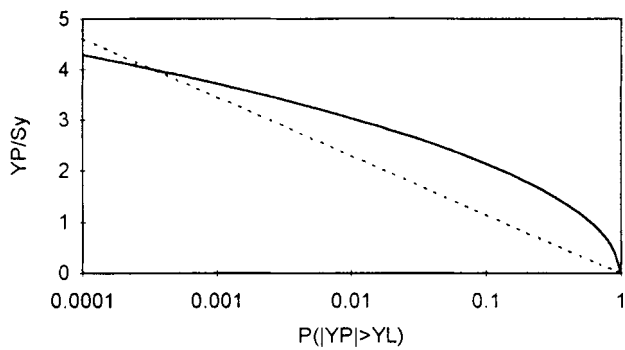

FIGURE 11.8 Probability of exceedance functions for peaks in the displacement response cycles of band-limited (dashed curve) and narrow-band (solid curve) random vibration.

STATISTICAL ENERGY ANALYSIS

Statistical energy analysis (SEA) models the vibration response of a complex system as a statistical interaction between groups of modes associated with subsections of

the system. While the theoretical development of SEA has its roots in the field of random vibration, it does not require a random excitation for the statistical analysis. Instead, SEA uses the random variation of modal responses in complex systems to obtain statistical response predictions in terms of mean values and variances of the responses. Theoretically, the statistical averaging is over ensembles of nominally identical systems. However, in practice many systems have enough inherent complexity that the variation in the response over frequency and location is adequately represented by the ensemble statistics.

This is seen even in the relatively simple case of the distribution of bending modes in a simply-supported rectangular flat plate (Fig. 11.9). The resonance frequencies of the modes are given by

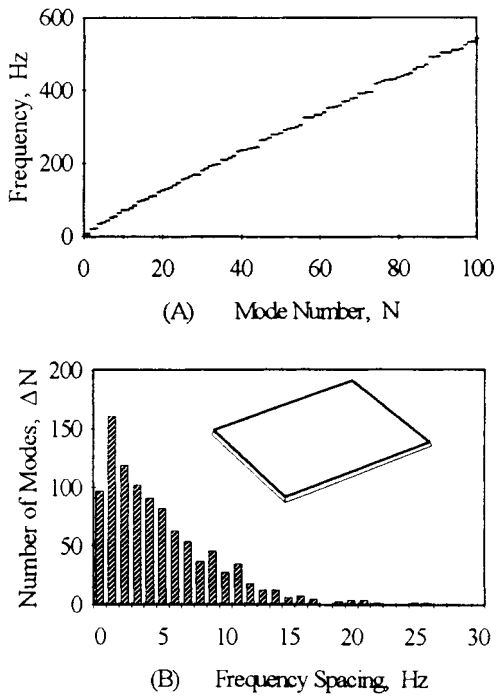

FIGURE 11.9 Mode count of a 2.6- × 2.4- × 0.01-meter simply supported, steel plate. (*A*) Resonance frequencies. (*B*) Distribution of resonance frequency spacings.

$$f_{m,n} = \left(\frac{\pi}{4\sqrt{3}}\right) h c_L \left[\left(\frac{m}{L_1}\right)^2 + \left(\frac{n}{L_2}\right)^2\right] \tag{11.56}$$

where L_1 and L_2 are the length dimensions, h is the thickness, c_L is the longitudinal wave speed of the plate material, and m and n are integers. The resonance frequencies are seen to follow approximately along a straight line. This slope of this line is the *average frequency spacing* $\overline{\delta f}$ (inverse of modal density per Hz) given by

$$\overline{\delta f} = \frac{h c_L}{\sqrt{3} L_1 L_2} \tag{11.57}$$

One way to represent the variation in the actual resonant frequencies is to plot the distribution in the frequency difference between two successive resonances, which can be plotted as shown in Fig. 11.9*B*. This distribution appears to be Poisson. Repeating this analysis for other plates with the same surface area, thickness, and material (thus having the same $\overline{\delta f}$), but with different values of L_1 and L_2, gives essentially the same results. This indicates that one way of looking at the modes of any one particular plate is to consider it as one realization from an ensemble of plates having the same statistical distribution of resonances. SEA uses this model to develop estimates of the vibration response of systems based on averages over the ensemble of similar systems. However, since the modes are usually a function of the parameter (fL/c), variations in the frequency f in a complex system often have the same statistics as variations in L (dimensions) and c (material properties) in an ensemble of similar systems.

The statistical model of a system is useful in a variety of applications. In the preliminary design phase of a system SEA can be used to obtain quantitative estimates of the vibration response even when all of the details of the design are not completely specified. This is because preliminary SEA estimates can be made using the general characteristics of the system components (overall size, thickness, material properties, etc.) without requiring the details of component shapes and attachments.

SEA is also useful in diagnosing vibration problems. The SEA model can be used to identify the sources and transfer paths of the vibrational energy. When measured data is available, SEA can help to interpret the data, and the measured data can be used to improve the accuracy of a preliminary SEA model. Since the SEA model gives quantitative predictions based on the physical properties of the system, it can be used to evaluate the effectiveness of design modifications. It can also be used with an optimization routine to search for improved design configurations.

SEA MODELING OF SYSTEMS

The statistical energy analysis (SEA) model of a complex system is based on the statistical analysis of the coupling between groups of resonant modes in subsections of the system. The modal coupling is based on the analysis of two coupled resonators as shown in Fig. 11.10. This is a more general case of the two degree-of-freedom system analyzed for a random vibration (see Fig. 11.7). Here there are two distinct res-

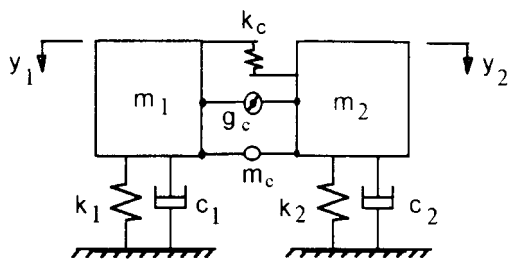

FIGURE 11.10 Two linear, coupled resonators, with displacement *y,* mass *m,* stiffness *k,* damper *c,* and gyroscopic parameter *g.*

onators coupled by stiffness, inertial, and gyroscopic interactions (represented by k_c, m_c, and g_c, respectively). If the two resonators are excited by different broad-band force excitations, then the net power flow between them through the coupling is given by

$$\begin{aligned}\Pi_{12} &= -k_c\,\overline{y_2\dot{y}_1} - g_c\,\overline{\dot{y}_2\dot{y}_1} + \frac{1}{4}m_c\,\overline{\ddot{y}_2\dot{y}_1} \\ &= B\,(E_1 - E_2)\end{aligned} \tag{11.58}$$

where

$$B = \frac{(2\pi\mu)^2}{d}[\Delta_1 f_2^4 + \Delta_2 f_1^4 + f_1 f_2(\Delta_1 f_2^2 + \Delta_2 f_1^2)]$$

$$+\frac{1}{d}[(\gamma^2 + 2\mu\kappa)(\Delta_1 f_2^2 + \Delta_2 f_1^2) + \kappa^2(\Delta_1 + \Delta_2)]$$

$$E_i = (m_i + m_c/4)\overline{\dot{y}_i^2}$$

and

$$d = (1-\mu^2)[(2\pi)^2(f_1^2 - f_2^2)^2 + (\Delta_1 + \Delta_2)(\Delta_1 f_2^2 + \Delta_2 f_1^2)]$$

$$\Delta_i = \frac{c_i}{(m_i + m_c/4)}$$

$$f_i^2 = \frac{(1/2\pi)^2(k_i + k_c)}{(m_i + m_c/4)}$$

$$\mu = \left(\frac{m_c}{4}\right)\left(\frac{m_1 + m_c}{4}\right)^{-1/2}\left(\frac{m_2 + m_c}{4}\right)^{-1/2}$$

$$\gamma = g_c\left(\frac{m_1 + m_c}{4}\right)^{-1/2}\left(\frac{m_2 + m_c}{4}\right)^{-1/2}$$

$$\kappa = k_c\left(\frac{m_1 + m_c}{4}\right)^{-1/2}\left(\frac{m_2 + m_c}{4}\right)^{-1/2}$$

This result can be interpreted by defining the two individual uncoupled resonators as the subsystems that exist when one of the degrees-of-freedom is constrained to zero. For either uncoupled resonator the kinetic energy averaged over a cycle, $(m + m_c/4)\overline{\dot{y}_i^2}/2$, is equal to the average potential energy, $(k + k_c)\overline{y_i^2}/2$. Equation (11.58) can then be seen to state two important results: (1) the power flow is proportional to the difference in the vibrational energies of the two resonators, and (2) the coupling parameter B is positive definite and symmetrical so the system is reciprocal and power always flows from the more energetic resonator to the less energetic one. As a corollary, when only one resonator is directly excited, the maximum energy level of the second resonator is that of the first resonator.

It should be noted that this analysis is exact for a coupling of arbitrary strength as long as there is no dissipation in the coupling. Even when there is dissipation in the coupling, this analysis is approximately correct as long as the coupling forces due to

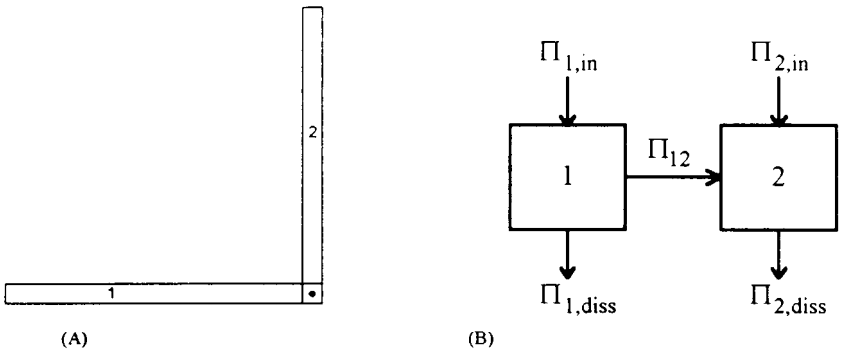

FIGURE 11.11 Modeling of distributed systems. (*A*) Two coupled beams. (*B*) SEA model of two coupled subsystems with power flow Π.

the dissipation are small compared to the other coupling forces. In practice when systems have interface damping at the connections between subsystems (such as in bolted or spot welded joints), the associated damping can be split between subsystems and the interface considered damping free.

As an example of how this analysis is extended to a distributed system, consider the two coupled beams in Fig. 11.11*A*. The modes of the system can be obtained from an eigenvalue solution of the complete system, or they can be obtained from a coupled pair of equations for the individual (or uncoupled) straight beam subsystems. The latter case leads to coupled mode equations similar to the ones used for the two coupled resonators. However, in this case each mode in one beam subsystem is coupled to all of the relevant modes in the other beam subsystem. The total power flow between the two beam subsystems is then the sum of the individual mode-to-mode power flows.

If the significant coupling is assumed to occur in a limited frequency range Δf (a good assumption for $\zeta << 1$ and $\Delta f >> \zeta f$), then the average net power flow can be found by averaging the value of B over Δf and using average beam subsystem modal energies in Eq. (11.58). This gives

$$\Pi_{12} = \overline{B} N_1 N_2 \left(\frac{E_1}{N_1} - \frac{E_2}{N_2} \right) \tag{11.59}$$

with

$$\overline{B} = \frac{1}{4\Delta f} \left[\mu^2 (2\pi f)^2 + (\gamma^2 + 2\mu\kappa) + \frac{\kappa^2}{(2\pi f)^2} \right]$$

where N_1 and N_2 are the number of modes in the two beam subsystems with resonance frequencies in Δf.

For either beam the total vibrational energy is $E_i = m_i \overline{\dot{y}_i^2}$, where m_i is the total mass of the beam and $\overline{\dot{y}_i^2}$ is the mean-square velocity averaged over space and time. Equation (11.59) shows that the power flow between two distributed subsystems is proportional to the difference in the average *modal* energies E_i/N_i, not the difference in the total energies (which are proportional to the vibration level). This means it is possible for a thick beam with fewer resonant modes in a frequency band and a

lower vibration level to be the source of power for a connected thinner beam with more resonant modes and a higher vibration level.

A more useful form of Eq. (11.59) is obtained by defining a *coupling loss factor* $\eta_{12} \equiv \overline{B}N_2/(2\pi f)$ (and by reciprocity $\eta_{21} \equiv N_1\eta_{12}/N_2$). The coupling loss factor is analogous to the *damping loss factor* for a subsystem defined by $\eta_i = 2\zeta_i$. The coupling loss factor is a measure of the rate of energy lost by a subsystem through coupling to another subsystem, whereas the damping loss factor is a measure of the rate of energy lost through dissipation. The average power flow is then given by

$$\Pi_{12} = 2\pi f(\eta_{12}E_1 - \eta_{21}E_2) \tag{11.60}$$

Using the equivalent expression for the power dissipated in each subsystem, $\Pi_{i,\text{diss}} = 2\pi f\eta_i E_i$, along with the result from Eq. (11.38) for the transient response of a resonator, the following set of equations can be written for the conservation of energy between two coupled subsystems ($\Pi_{\text{in}} = \Pi_{\text{out}} + dE/dt$):

$$\begin{aligned} \Pi_{1,\text{in}} &= 2\pi f(\eta_1 + \eta_{12})E_1 - 2\pi f\eta_{21}\,E_2 + \frac{dE_1}{dt} \\ \Pi_{2,\text{in}} &= -2\pi f\eta_{12}E_1 + 2\pi f(\eta_2 + \eta_{21})E_2 + \frac{dE_2}{dt} \end{aligned} \tag{11.61}$$

where $\Pi_{i,\text{in}}$ is used to denote power supplied by external sources. The SEA block diagram for this power flow model of two coupled subsystems is shown in Fig. 11.11*B*. These equations are first-order differential equations for the diffusion of energy between subsystems. They are in a form analogous to heat flow or fluid potential flow problems. For steady-state problems the dE/dt terms are zero.

For narrow-band analysis, the SEA equations can be used to obtain averages in the response of the system over frequency. In this case it is more convenient to use the average frequency spacing between modes $\overline{\delta f} = \Delta f/N$ as the mode count in Eq. (11.59). This gives

$$\overline{\Pi_{12}} = \frac{2\pi f}{\overline{\delta f_1}}\eta_{12}(E_1\overline{\delta f_1} - E_2\overline{\delta f_2}) \tag{11.62}$$

The terms $2\pi E_i\overline{\delta f_i}$ have units of power and are called the *modal power potential.*

The value of η_{12} is difficult to evaluate directly from $\overline{B}$ in practice. Instead, indirect methods are often used as described in the section "Coupling Loss Factors." The normalized variance in the value of η_{12} averaged over Δf for edge-connected subsystems is given by

$$\frac{\sigma_{\eta 12}{}^2}{\eta_{12}{}^2} = \frac{1}{\pi f\left(\dfrac{\eta_1}{\overline{\overline{\delta f_1}}} + \dfrac{\eta_2}{\overline{\overline{\delta f_2}}}\right) + \Delta f\left(\dfrac{1}{\overline{\overline{\delta f_1}}} + \dfrac{1}{\overline{\overline{\delta f_2}}}\right)} \tag{11.63}$$

The variance in the coupling depends primarily on the system *modal overlap factor* defined by $M_S = \pi f(\eta_1/\overline{\delta f_1} + \eta_2/\overline{\delta f_2})/2$, which is the ratio of the effective modal bandwidth to the average modal frequency spacing. When the system modal overlap factor is less than 1, the variance is larger than the square of the mean value, which may be unacceptably large. This indicates why SEA models tend to converge better with measured results at frequencies above where $M_S = 1$.

Note that the modal overlap in each uncoupled subsystem does not have to be large in order for the variance in the coupling to be small. In fact the SEA model can be used to evaluate the response of a single resonator mode attached to a vibrating flat plate as illustrated in Fig. 11.12. The power flow equations in the form of Eq.

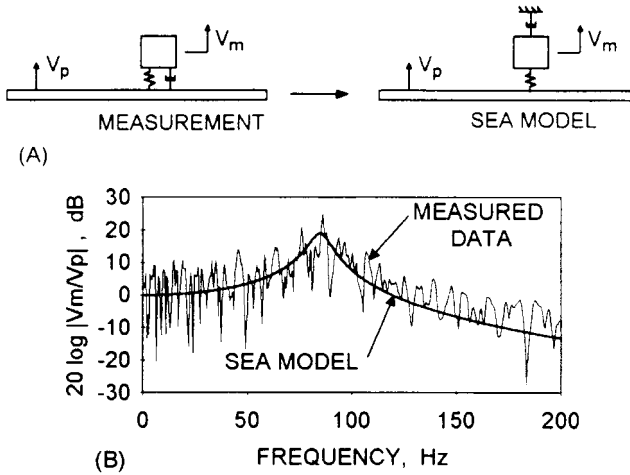

FIGURE 11.12 Response of a resonator with vibration V_m, mounted on a plate with vibration V_p. (*A*) Comparison of the measurement configuration and the SEA model. (*B*) Comparison of the measured response and the SEA predictions.

(11.59) are used. The uncoupled resonator has one mode at $f_2 = \sqrt{k_2/m_2}$, so $N_2 = 1$. The mean-square vibration velocity level of the plate in a frequency band Δf encompassing f_2 is $\dot{y}_1^2 = W_{\dot{y}1}(f)\Delta f$. The average number of plate modes resonating in this frequency band is $N_1 = \Delta f/\delta f_1$. The coupling loss factor is evaluated to be

$$\eta_{21} = \frac{\pi}{2}\frac{f_2}{\delta f_1}\frac{m_2}{m_1} \tag{11.64}$$

Since $\Pi_{12} = \Pi_{2,\text{diss}}$, the mean-square response of the resonator mass is given by

$$\overline{\dot{y}_2^2} = \frac{\pi}{2}\frac{f_2 W_{\dot{y}1}(f)}{\eta_{21} + \eta_2} \tag{11.65}$$

Even if the resonator damping goes to zero, its maximum energy level is limited to the average modal energy in the plate:

$$m_2\,\overline{\dot{y}_2^2}_{,\max} = m_1 W_{\dot{y}1}(f)\Delta f \tag{11.66}$$

If the resonator energy momentarily gets higher, it transmits the energy back into the plate. Therefore, the plate acts both as a source of excitation and as a dissipator of energy for the resonator. The effective loss factor for the resonator is $\eta_{21} + \eta_2$.

The frequency response function for the resonator can then be evaluated using Eq. (11.34). Figure 11.12*B* compares this result with the measured narrow-band frequency spectrum of a 0.1-kg mass attached to a 2.5-mm steel plate with a resilient mounting having negligible damping and $f_2 = 85$ Hz. The measured response of the mass is multimodal since the resonator responds as a part of all of the modes of the coupled system. However, the statistical average response curve accurately represents the multimodal response. The normalized variance of the narrow-band SEA response calculation is estimated from Eq. (11.63) to be 0.5.

For larger systems the following procedure can be used to develop a complete SEA model of the system response to an excitation:

1. Divide the system into a number of coupled subsystems.
2. Determine the mode counts and damping loss factors for the subsystems.
3. Determine the coupling factors between connected subsystems.
4. Determine the subsystem input powers from external sources.
5. Solve the energy equations to determine the subsystem response levels.

The steps in this procedure are described in the following sections of this chapter. When used properly, the SEA model will calculate the distribution of vibration response throughout a system as a result of an excitation. The response distribution is calculated in terms of a mean value and a variance in the vibration response of each subsystem averaged over time and the spatial extent of the subsystem.

MODE COUNTS

In this section the mode counts for a number of idealized subsystem types are given in terms of the average frequency spacing $\overline{\delta f}$ between modal resonances. Experimental and numerical methods for determining the mode counts of more complicated subsystems are also described.

The mode count is sometimes represented by the average number of modes, N or ΔN, resonating in a frequency band, and sometimes by the modal density, represented in cyclical frequency as $n(f) = dN/df$. These are related to the average frequency spacing by

$$n(f) = \frac{1}{\overline{\delta f}} \simeq \frac{\Delta N}{\Delta f} \tag{11.67}$$

For a one-dimensional subsystem, such as a straight beam or bar, with uniform material and cross-sectional properties and with length L, the average frequency spacing between the modal resonances is given by

$$\overline{\delta f}^{1D} = \frac{c_g}{2L} \tag{11.68}$$

where c_g is the energy group speed for the particular wave type being modeled.

For longitudinal waves c_g is equal to the phase speed $c_L = \sqrt{E/\rho}$, where E is the elastic (Young's) modulus and ρ is the density of the material. For torsional waves c_g is equal to the phase speed $c_T = \sqrt{GJ/\rho I_p}$, where G is the shear modulus of the material, and J and I_p are the torsional moment of rigidity and polar area moment of inertia, respectively, of the cross section. For beam bending waves (with wavelengths

long compared to the beam thickness) the group speed is twice the bending phase speed c_B, or $c_g = 2c_B = 2\sqrt{2\pi f \kappa c_L}$, where κ is the radius of gyration of the beam cross section. For a beam of uniform thickness h, $\kappa = h/\sqrt{12}$.

For a two-dimensional subsystem, such as a flat plate, with uniform thickness and material properties and with surface area A, the average frequency spacing between the modal resonances is given by

$$\overline{\delta f}^{2D} = \frac{c_p c_g}{2\pi f A} \tag{11.69}$$

where c_p is the phase speed for the particular wave type being modeled. For plate bending waves (with wavelengths long compared to the plate thickness) $c_g = 2c_p = 2c_{B'} = 2\sqrt{2\pi f \kappa c_{L'}}$, where κ is the radius of gyration, $c_{L'} = \sqrt{E/\rho(1-\mu^2)}$, and μ is Poisson's ratio. For in-plane compression waves $c_g = c_p = c_{L'}$. For in-plane shear waves $c_g = c_p = c_S = \sqrt{G/\rho}$.

For a three-dimensional subsystem, such as an elastic solid, with uniform material properties and with volume V, the average frequency spacing between the modal resonances is given by

$$\overline{\delta f}^{3D} = \frac{c_o^3}{4\pi f^2 V} \tag{11.70}$$

where c_o is the ambient shear or compressional wave speed in the medium.

For more complicated subsystems the mode counts can be obtained in a number of other ways. Generally, the mode counts only need to be determined within an accuracy of 10 percent in order for any resulting error to be less than 1 dB in the SEA model. For more complicated wave types, such as bending in thick beams or plates, the formulas given above for $\overline{\delta f}$ can be used with the correct values of c_g and c_p obtained from the dispersion relation for the medium.

For more complicated geometries a numerical solution, such as a finite element model, can be used to determine the eigenvalues of the subsystem. Then, the values of $\overline{\delta f}$ can be obtained using Eq. (11.67). In this case it is often necessary to average the mode count over a number of particular geometric configurations or boundary conditions in order to obtain an accurate estimate of the average modal spacing.

When a physical sample of the subsystem exists, experimental data can be used to estimate or validate the mode count. For large modal spacing (small modal overlap) the individual modes can sometimes be counted from a frequency response measurement. However, this method usually undercounts the modes because some of them may occur paired too closely together to be distinguished. An alternate experimental procedure is to use the relation between the mode count and the average mobility of a structure:

$$\overline{\delta f} = \frac{1}{4m\overline{G}} \tag{11.71}$$

where m is the mass of the subsystem and $\overline{G}$ is the average real part of the mechanical mobility (ratio of velocity to force at a point excitation; see Chap. 10). As with the numerical method, the experimental measurement should be averaged over a variation in the boundary condition used to support the subsystem since no one static support accurately represents the dynamic boundary condition the subsystem sees when it is part of the full system. Also the measurement of $\overline{G}$ should be averaged over several excitation points.

DAMPING LOSS FACTORS

In this section typical methods for determining the damping loss factor of subsystems are given along with some typical values used in statistical energy analysis (SEA) models of complex structures. The damping in SEA models is usually specified by the loss factor which is related to the critical damping ratio ζ and the quality factor Q by

$$\eta = 2\zeta = \frac{1}{Q} \tag{11.72}$$

Chapters 36 and 37 describe the damping mechanisms in structural materials and typical damping treatments. In complex structures the structural material damping is usually small compared to the damping due to slippage at interfaces and added damping treatments. Because the level of added damping is so strongly dependent on the details of the application of a damping treatment, measurements are usually needed to verify analytical calculations of damping levels.

One method to measure the damping of a subsystem is the decay rate method, where the free decay in the vibration level is measured after all excitations are turned off. The initial decay rate DR (in dB/sec) is proportional to the total loss factor for the subsystem:

$$\eta = \frac{DR}{27.3f} \tag{11.73}$$

If the subsystem is attached to other structures, the coupling loss factors will be included in the total loss factor value. Therefore, the subsystem must be tested in a decoupled state. On the other hand, if the connection interfaces provide significant damping due to slippage, then these interfaces must be simulated in the damping test.

Another method of measuring the damping is the half-power bandwidth method illustrated in Fig. 2.22. The width of a resonance Δf in a frequency response measurement is measured 3 dB down from the peak and the damping is determined by

$$\eta = \frac{\Delta f}{f_n} \tag{11.74}$$

As with other measurements of subsystem parameters, the damping measurements must be averaged over multiple excitation points with a variety of boundary conditions.

For preliminary SEA models an empirical database of damping values is useful for initial estimates of the subsystem damping loss factors. Figure 11.13 is an illustration of the typical damping values measured in steel and aluminum machinery structures for different construction methods and different applied damping treatments.

The initial estimates of damping levels in a preliminary SEA model can be improved if measurements of the spatial decay of the vibration levels in the system are available. The spatial decay calculated in the SEA model is quite strongly dependent on the damping values used. Therefore, an accurate estimate of the actual damping can be obtained by comparing the SEA calculations to the measured spatial decay (assuming the other model parameters are correct).

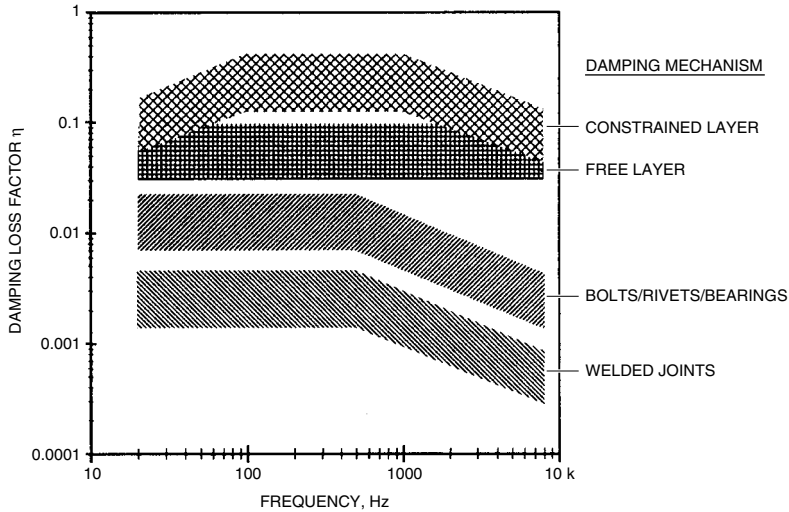

FIGURE 11.13 Empirical values for the damping loss factor η in steel and aluminum machinery structures with different damping mechanisms (assumed to be efficiently applied, but in less than ideal laboratory conditions).

COUPLING LOSS FACTORS

The coupling loss factor is a parameter unique to statistical energy analysis (SEA). It is a measure of the rate of energy transfer between coupled modes. However, it is related to the transmission coefficient τ in wave propagation. This can be illustrated with the system shown in Fig. 11.14. For a wave incident on a junction in subsystem

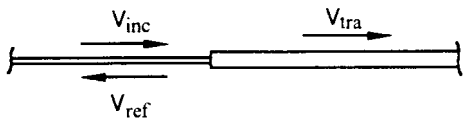

FIGURE 11.14 Evaluation of the coupling loss factor using a wave transmission model for an incident wave V_{inc} at a junction, resulting in a reflected wave V_{ref} and a transmitted wave V_{tra}.

1 with incident power Π_{inc}, the power transmitted to subsystem 2, Π_{tra}, is by definition of the transmission coefficient τ_{12} given by

$$\Pi_{tra} = \tau_{12}\Pi_{inc} \tag{11.75}$$

In addition, the junction reflects some power, Π_{ref}, back into subsystem 1 given by

$$\Pi_{ref} = (1 - \tau_{12})\Pi_{inc} \tag{11.76}$$

assuming there is no power dissipated at the junction. The energy density in subsystem 1 is given by $E_1' = c_{g_1}(\Pi_{inc} + \Pi_{ref})$. The corresponding SEA representation of the system is

$$\Pi_{tra} = \Pi_{1 \to 2} = 2\pi f \eta_{12} E_1 \tag{11.77}$$

For a subsystem of length L_1, $\overline{\delta f_1} = c_{g_1}/(2L_1)$ and $E_1 = L_1 E_1'$. Solving for the coupling loss factor gives

$$\eta_{12} = \frac{\overline{\delta f_1}}{\pi f} \frac{\tau_{12}}{2 - \tau_{12}} \tag{11.78}$$

A more detailed analysis indicates that this result is valid for point connections in a system with a modal overlap greater than 1. If the system has a constant modal frequency spacing $\overline{\delta f}$, then the Nth mode will occur at $f = N\overline{\delta f}$. If the damping loss factor is η, the system modal overlap is given by $M_S = \pi\eta f/(2\overline{\delta f})$. Then the modal overlap is greater than 1 for frequencies $f > 2\overline{\delta f}/(\pi\eta)$ or for mode numbers $N > 2/(\pi\eta)$. SEA is still valid below this frequency and mode number, but the variance of the model calculations (and in the measured frequency response functions) becomes large.

For point-connected subsystems the transmission coefficient can be evaluated from the junction impedances:[4]

$$\tau_{12} = \frac{4R_1R_2}{|Z_1 + Z_2|^2} \tag{11.79}$$

where R_i is the real part of the impedance Z_i (ratio of force to velocity at a point excitation) at the junction attachment point of subsystem i. When more than two subsystems are connected at a common junction, the denominator of Eq. (11.79) must include the sum of all impedances at the junction.

For subsystems with line and area junctions the analysis of the coupling loss factor is complicated by the distribution of angles of the waves incident on the junction. However, approximate results have been worked out for many important cases. Eq. (11.78) can be generalized for all cases as

$$\eta_{12} = \frac{\overline{\delta f_1}}{\pi f} \frac{I_{12}\tau_{12}(0)}{2 - \tau_{12}(0)} \tag{11.80}$$

where $\tau_{12}(0)$ is the normal incidence transmission coefficient for waves traveling perpendicular to the junction, and I_{12} contains the result of an average over all angles of incidence.

For line-connected plates the coupling loss factor between bending modes is found using

$$I_{12} = \frac{L_j}{4} \left(\frac{k_1^4 k_2^4}{k_1^4 + k_2^4} \right)^{1/4} \tag{11.81}$$

where L_j is the length of the junction and $k_i = 2\pi f/c_{Bi}$ is the wave number of the modes in subsystem i.

When experimental verification of the evaluation of the coupling loss factor is desired, measurements similar to those used for damping can be used. A decay rate measurement of a subsystem connected to another (heavily damped) subsystem will give a loss factor equal to the sum of the damping and coupling loss factor for the first subsystem. Alternately, subsystem 1 can be excited alone and the spatially averaged response levels of the two connected subsystems can be measured. Using $\Pi_{12} = \Pi_{2,diss}$, the coupling loss factor is found from

$$\eta_{12} = \frac{\eta_2 E_2}{E_1 - \overline{\delta f_2} E_2 / \overline{\delta f_1}} \tag{11.82}$$

This result indicates a potential problem in determining the coupling loss factor from measured results. If $E_2\overline{\delta f_2} \simeq E_1\overline{\delta f_1}$, then taking the difference between their values in Eq. (11.82) will greatly magnify the experimental errors in determining the parameters used in this formula. This indicates why it is mathematically unstable to use measured levels in a multiple subsystem model to back calculate the coupling loss factors. However, good results can be obtained for a single junction between two subsystems if one is excited and the other is artificially damped in order to increase difference between $E_1\overline{\delta f_1}$ and $E_2\overline{\delta f_2}$. Figure 11.15 shows the results of an experimen-

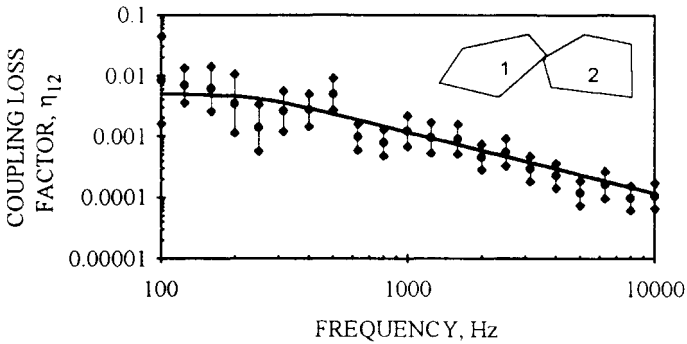

FIGURE 11.15 Coupling loss factor η_{12} for point connected plates; ◆—◆ measured data with 95 percent confidence intervals; —— calculated values using Eqs. (11.80) and (11.81).

tal validation of Eqs. (11.80) and (11.81) for the coupling loss factor between two plates connected at a point. The experimental error is also included, which even in this idealized laboratory environment is more than 50 percent. While the *back calculation* of the coupling loss factors tends to be unstable, the forward calculation in the SEA model is relatively insensitive to errors in the coupling loss factor values, making the model fairly robust.

MODAL EXCITATIONS

The power put into subsystem modes by the system excitations is needed in order to use the statistical energy analysis (SEA) model for calculations of absolute response levels. The mode counts, damping, and coupling loss factors can be used to evaluate relative transfer functions in the system for a unit input power. However, for actual response-level calculations the modal input power from the actual excitation sources must be calculated.

For a point force excitation $F(t)$ the average power put into a system is

$$\Pi_{in} = \overline{F^2}\ \overline{G} \tag{11.83}$$

where $\overline{G}$ is the average real part of the mobility at the excitation point. For a prescribed point velocity source $\dot{y}(t)$ the average power put into a system is

$$\Pi_{\text{in}} = \overline{\dot{y}^2}\,\overline{R} \tag{11.84}$$

where $\overline{R}$ is the average real part of the impedance at the excitation point.

The normalized variance in the input power due to variations in the mode shapes and frequency response function of the system is approximated by

$$\frac{\sigma_{\Pi_{\text{in}}}{}^2}{\Pi_{\text{in}}{}^2} = \frac{3\overline{\delta f}}{\pi f \eta + \Delta f} \tag{11.85}$$

where Δf is the bandwidth of the excitation. For more complicated excitations the input power can be estimated by measuring the response of a system to the excitation and using the SEA model to back calculate the input power. Alternatively, the measured response levels of the excited subsystem can be used as "source" levels, and the power flow into the rest of the system can be evaluated using the SEA model.

SYSTEM RESPONSE DISTRIBUTION

To solve for the distribution of vibrational energy in a system it is convenient to rewrite Eq. (11.61) in symmetric form:

$$[B]\{\Phi\} + [I]\left\{\frac{dE}{dt}\right\} = \{\Pi_{\text{in}}\} \tag{11.86}$$

where $[I]$ is the identity matrix, $\{\Phi\} = 2\pi\{E/\overline{\delta f}\}$ is the vector of modal power potential, and $[B]$ is the symmetric matrix of coupling and damping terms with off-diagonal terms $B_{ij} = -f\,\eta_{ij}/\overline{\delta f_i}$ and diagonal terms $B_{ii} = (f/\overline{\delta f_i})(\eta_i + \Sigma_j\,\eta_{ij})$. This system of equations can be solved using standard numerical methods. Solving for the values of E gives a mean value estimate of the energy distribution.

The variance in E is more difficult to evaluate because it depends on the evaluation of the inverse matrix $[B]^{-1}$. If the variance of each term in $[B]$ is small compared to its mean-square value, then the variances in $[B]^{-1}$ can be approximated by

$$[\sigma_{B^{-1}}{}^2] \simeq [(B_{ij}{}^{-1})^2][\sigma_B{}^2][(B_{ij}{}^{-1})^2] \tag{11.87}$$

where the notation $[(B_{ij}{}^{-1})^2]$ refers to a matrix with the squares of the elements in $[B]^{-1}$, term for term.

The subsystem energy values can be converted to dynamic response quantities using the relation $E = m\overline{\dot{y}^2}$. For a narrow-band vibration at frequency f_c (which could be a single one-third octave band response in a broad-band analysis) the displacement response is $\overline{y^2} \simeq \overline{\dot{y}^2}/(2\pi f_c)^2$ and the acceleration response is $\overline{\ddot{y}^2} \simeq (2\pi f_c)^2\,\overline{\dot{y}^2}$. The relation between the vibration velocity response and the maximum dynamic strain depends on the type of motion involved. For longitudinal motion the mean-square strain is $\overline{\epsilon^2} = \overline{\dot{y}^2}/c_L{}^2$. For bending motion of a uniform beam or plate the maximum strain is $\overline{\epsilon_{\max}{}^2} = 3\overline{\dot{y}^2}/c_L{}^2$.

When the response values in a complex system are plotted on a logarithmic scale, a surprising result occurs. The log-values are distributed with an approximately Gaussian distribution over frequency. This is illustrated in Fig. 11.16 for a beam network. The system frequency response function is computed numerically using a transfer impedance model including bending and longitudinal and torsional motions

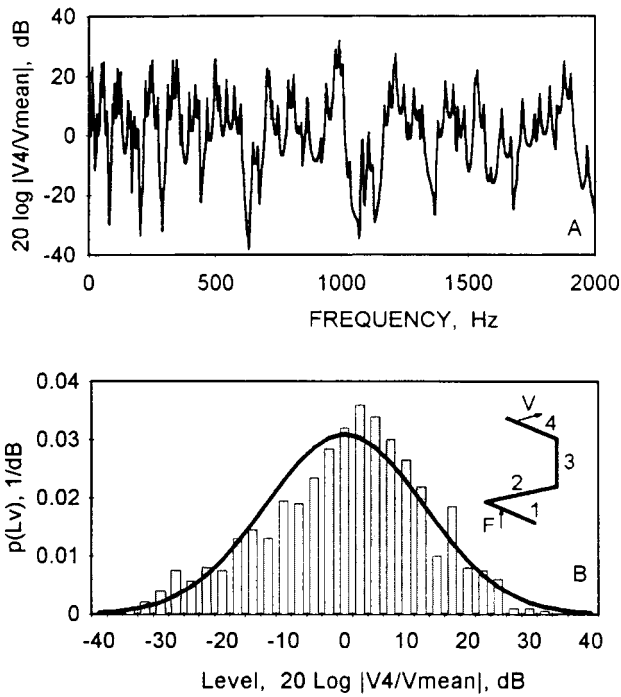

FIGURE 11.16 Numerical calculation of the vibration response of a four-beam network. (*A*) Normalized frequency response function for a point on beam 4. (*B*) Probability density function of log-levels, ▯ Numerical data histogram, — Normal distribution.

in each of the four beam segments. A histogram of the computed response values on the decibel scale compares very well with a Gaussian distribution. This result can be explained by noting that the response value at any particular frequency results from the product of a large number of quantities. Then the logarithm of the response value will be the sum of a large number of terms. If the complexity in the system causes the responses at different frequencies to be independent, then by the central limit theorem the log-values will tend to have a Gaussian distribution. This means that the mean-square response values will have a log-normal distribution.

The calculated mean values and variances in the SEA model can be converted to the decibel scale as follows. If the mean-square velocity $\overline{\dot{y}^2}$ has a log-normal distribution with variance $\sigma_{\dot{y}^2}{}^2$, then the velocity level $L_{\dot{y}} \equiv 10 \log_{10}(\overline{\dot{y}^2}/\dot{y}_{\text{ref}}{}^2)$ has a normal distribution with a mean value and variance given by

$$L_{\dot{y}} = 10 \log_{10}\left(\frac{\overline{\dot{y}^2}}{\dot{y}_{\text{ref}}^{\,2}}\right) - 5 \log_{10}\left[1 + \frac{\sigma_{\dot{y}^2}^{\,2}}{(\overline{\dot{y}^2})^2}\right]$$

$$\sigma_{L_{\dot{y}}}^{\,2} = 43 \log_{10}\left[1 + \frac{\sigma_{\dot{y}^2}^{\,2}}{(\overline{\dot{y}^2})^2}\right] \tag{11.88}$$

Note that the mean of the decibel levels is not equal to the decibel level of the mean-square value.

TRANSIENT (SHOCK) RESPONSE USING SEA

The statistical energy analysis (SEA) model can solve for the transient response of a system using Eq. (11.61). The numerical solution methods for equations of this form can be illustrated using the finite difference method. Given an initial energy state $E(0)$, the energy state at a short time later is approximated by

$$E(\Delta t) \simeq E(0) + \frac{dE}{dt}\,\Delta t \tag{11.89}$$

where $dE/dt = \Pi_{\text{in}} - \Pi_{\text{out}}$. This new energy distribution is then used to project forward to the next time step, etc. The accuracy of the solution depends on the size of Δt relative to the energy flow time constants in the system, $(2\pi f\eta)^{-1}$. For the finite difference solution, using $\Delta t \le (6\pi f\eta)^{-1}$ usually provides accurate results.

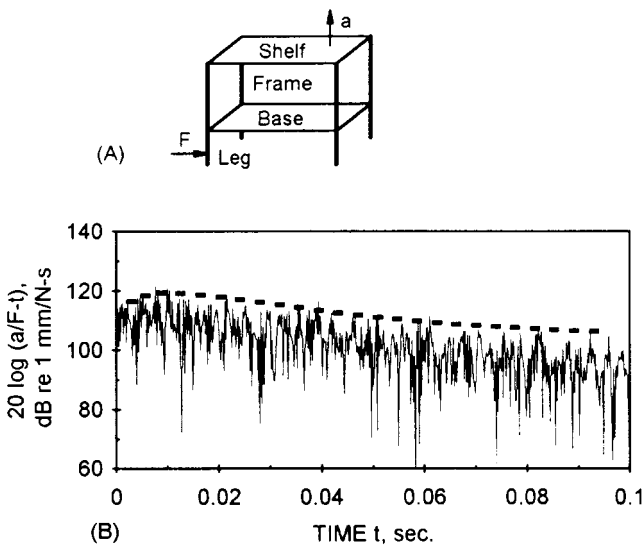

FIGURE 11.17 Transient response of an equipment shelf. (*A*) Experimental structure showing the locations of the impact *F* and the acceleration response *a*. (*B*) Comparison of the transient response of the structure; — Measured data, - - - SEA model.

An example of a transient analysis using SEA is shown in Fig. 11.17. The measured acceleration response of a shelf on an equipment rack for an impact at the leg is shown along with the corresponding transient SEA solution of Eq. (11.61). The energy level of the shelf builds up for the first 0.01 sec before beginning to decay.

Modeling the transient mean-square response with Eq. (11.39), the undamped shock spectrum for this response signal can be estimated using Eq. (11.42). Alternately, if a shock excitation is modeled as a time-dependent power input to the SEA model, then the peak response spectrum of the system components can be estimated directly from the maximum mean-square values in the transient SEA solution.

REFERENCES

1. Crandall, S. H., and W. D. Mark: "Random Vibration in Mechanical Systems," Academic Press, New York, 1963.
2. Lyon, R. H., and R. G. DeJong: "Theory and Application of Statistical Energy Analysis," 2d ed., Butterworth-Heinemann, Boston, Mass., 1995.
3. Caughey, T. K.: "Nonstationary Random Inputs and Responses," chap. 3, in S. H. Crandall (ed.), *Random Vibration,* vol. 2, M.I.T. Press, Cambridge, Mass., 1963.
4. Cremer, L., M. Heckl, and E. E. Ungar: "Structure-Borne Sound," 2d ed., Springer-Verlag, Berlin, 1988.